

## Supplement information

2

## 3 Large-scale assessment of oxic methane production in lakes using an isotopic 4 mass balance approach

5

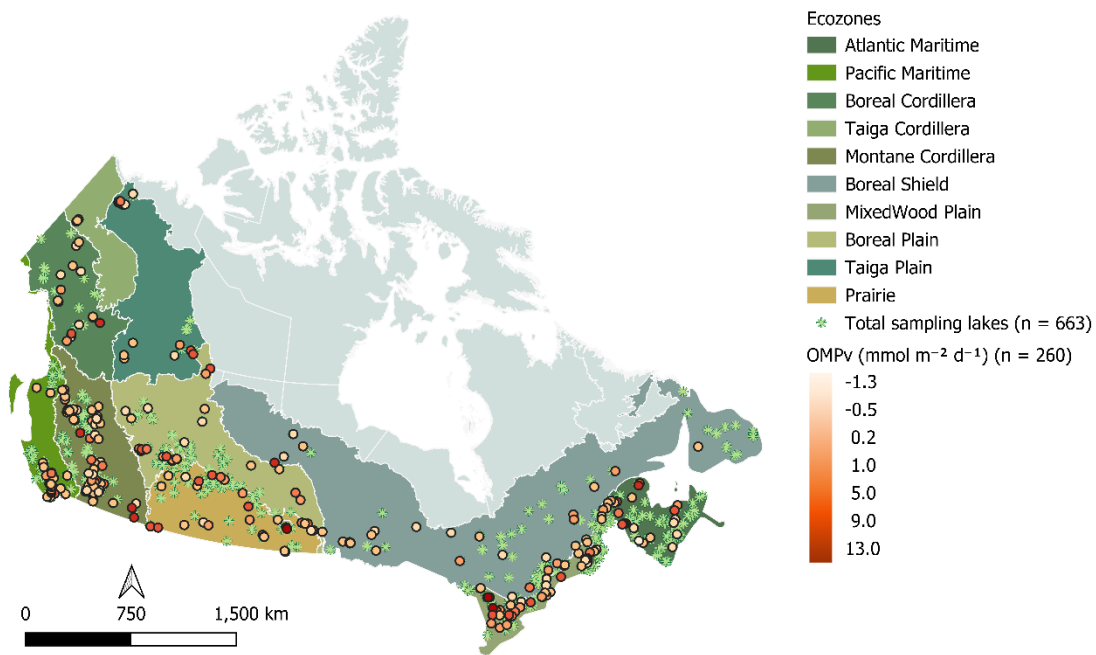
## 6 Authors and Affiliations

7 Jihyeon Kim<sup>\*1</sup>, Bruno Cremella<sup>2</sup>, Yannick Huot<sup>2</sup>, and Yves T. Prairie<sup>1</sup>

<sup>8</sup> <sup>1</sup>Département des sciences biologiques, Université du Québec à Montréal, Canada

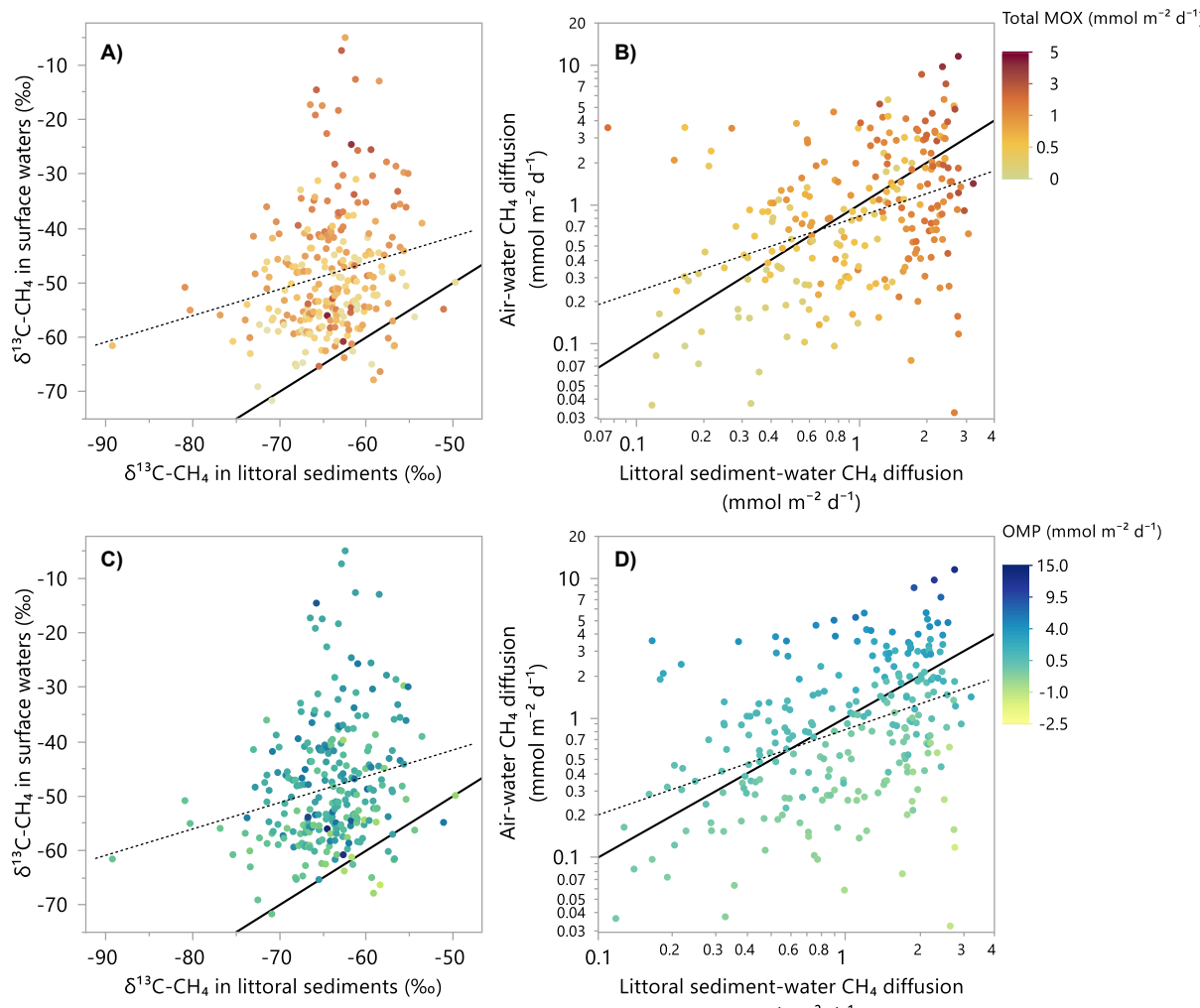
<sup>9</sup> <sup>2</sup>Département de géomatique appliquée, Université de Sherbrooke, Sherbrooke, Canada

10



11

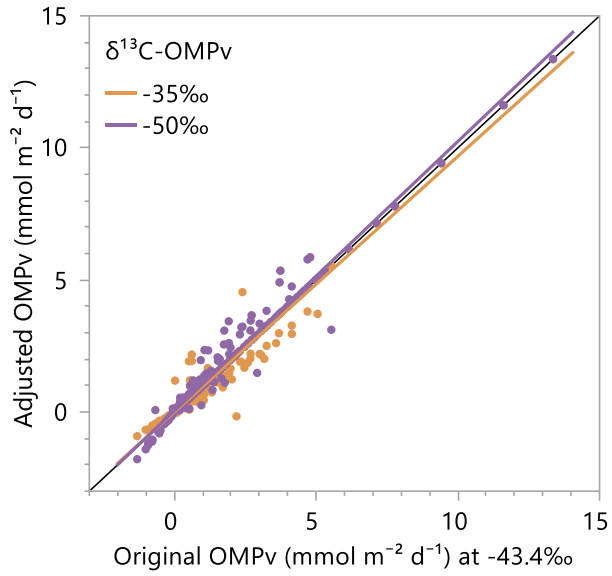
12 **Supplementary Fig. 1** | Map of sampling lakes, covering 10 provinces and 2 territories (42°N to 69°N and  
 13 52°W to 141°W) across Canada. As part of the national-scale lakes assessment (NSERC Lake Pulse  
 14 Project), a total of 663 lakes were sampled over three summers (2017 to 2019). Among them, OMPv rates  
 15 were estimated in 260 lakes with complete CH<sub>4</sub>-related measurements using our extended mass balance  
 16 approach.



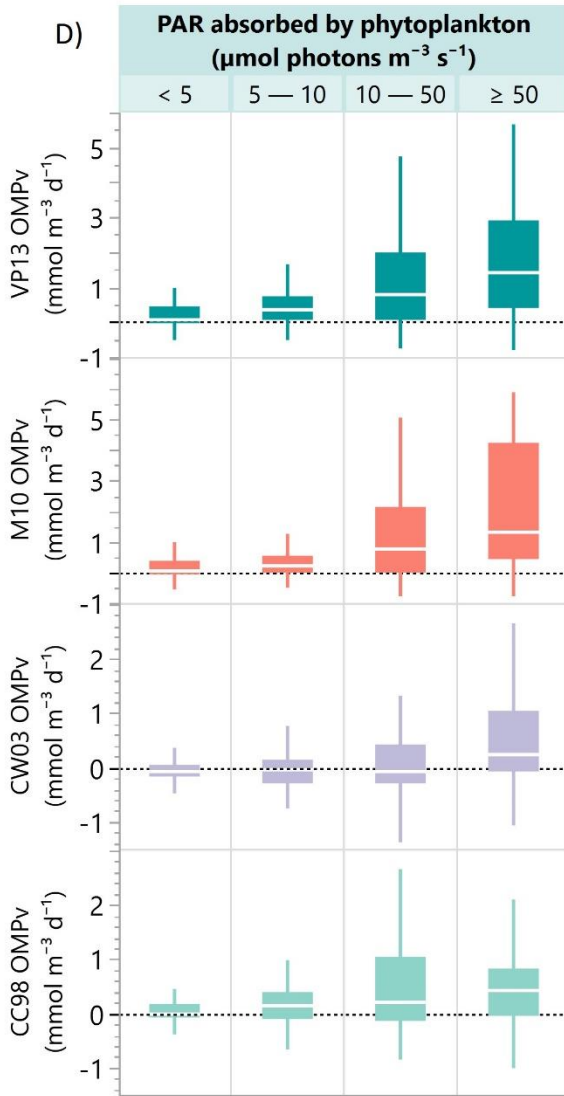
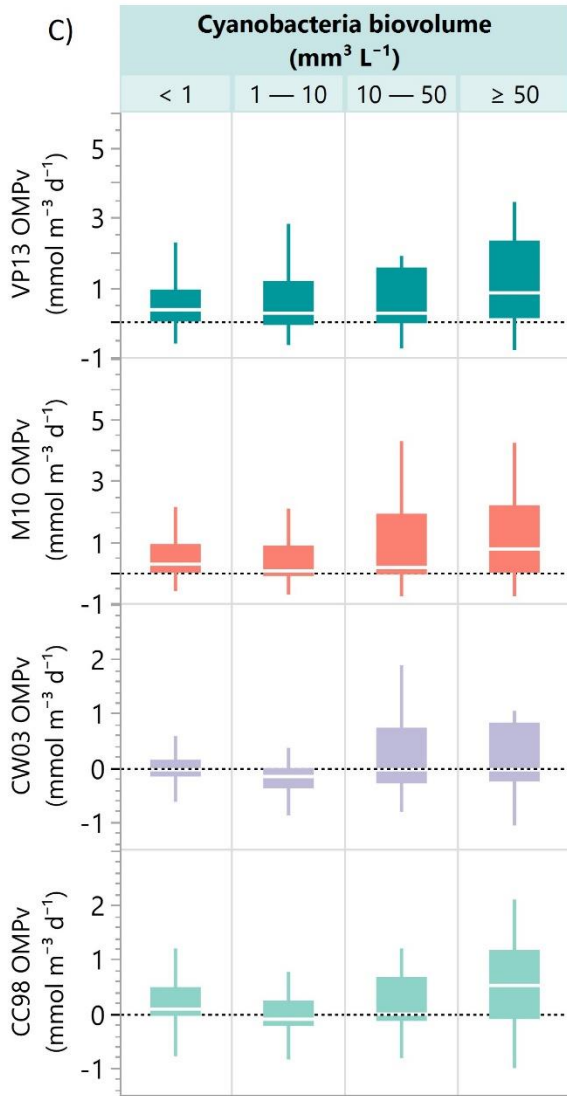
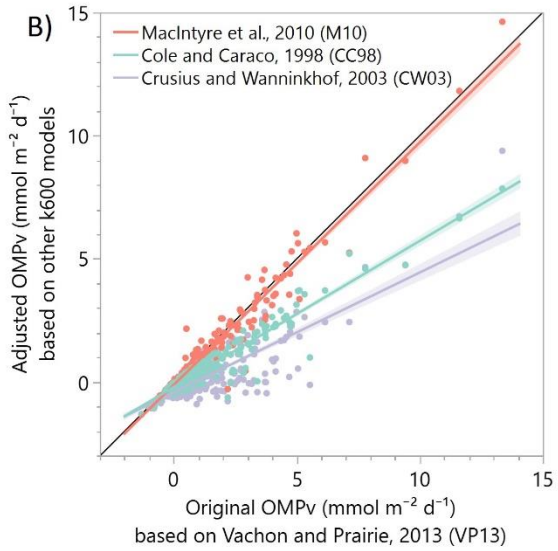
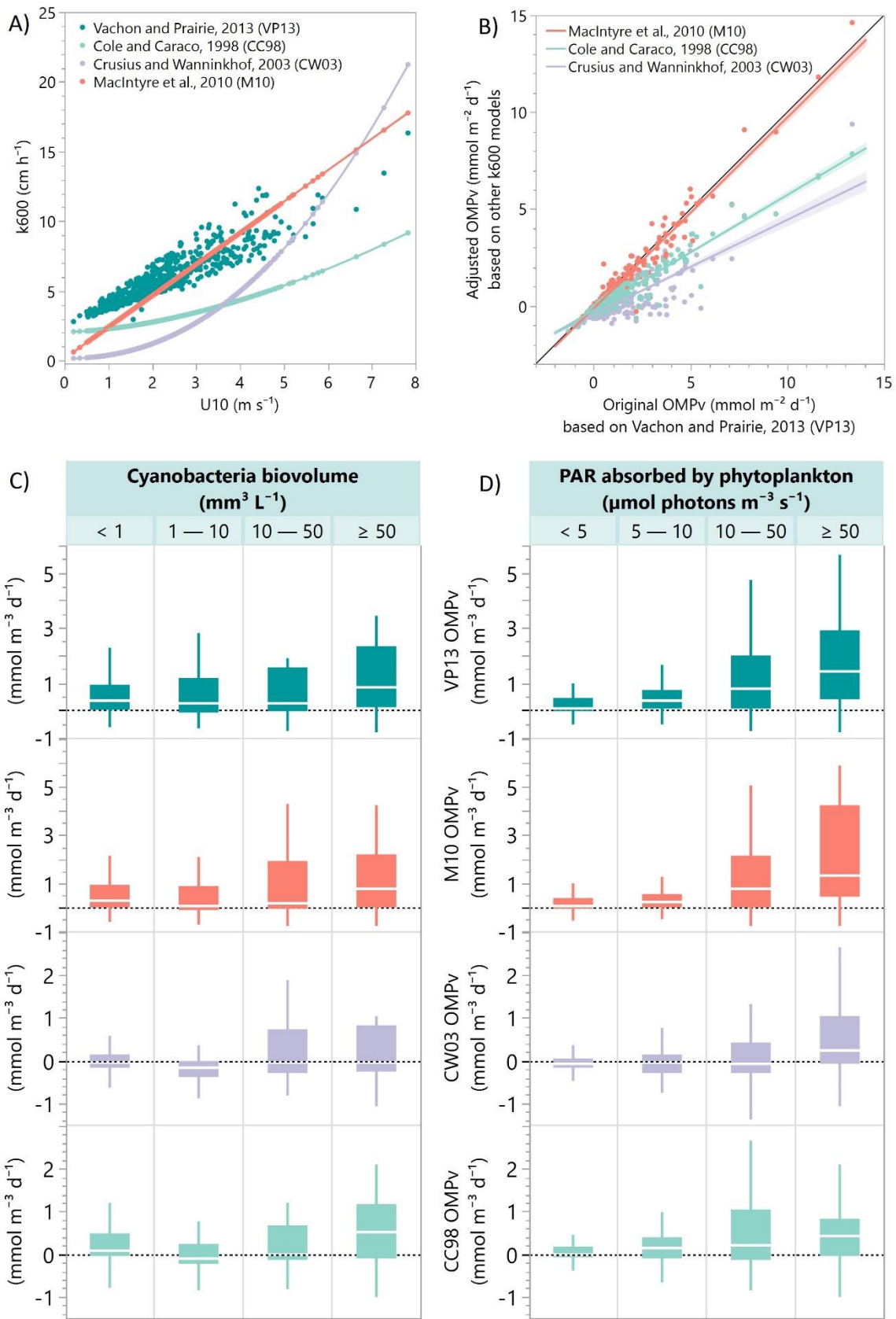
17

18 **Supplementary Fig. 2** | In line with Fig 1 of main context, our mass balance-based estimates of **A**) total  
 19 MOX and **B**) OMP further elucidate the quantitative mechanisms underlying the interplay between OMP  
 20 and total MOX as a key control on diffusive  $\text{CH}_4$  emissions to the atmosphere, beyond littoral sediment  
 21 inputs.

22

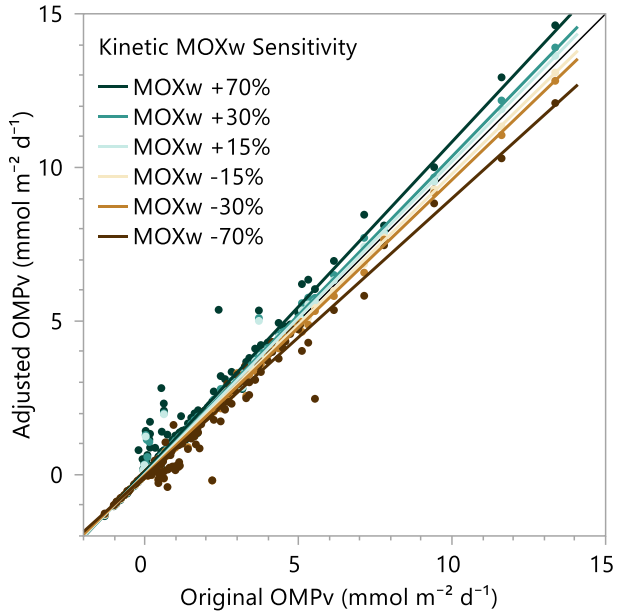


23 **Supplementary Fig. 3** | Sensitivity analysis of our mass balance to potential variability in  $\delta^{13}\text{C}_{\text{OMP}_V}$ . The x-  
24 axis shows  $\text{OMP}_V$  estimates assuming  $\delta^{13}\text{C}_{\text{OMP}_V} = -43.4\text{\textperthousand}$  (literature average), while the y-axis shows  
25 corresponding estimates when  $\delta^{13}\text{C}_{\text{OMP}_V}$  is adjusted to -35‰ and -50‰, respectively. The black line  
26 indicates the 1:1 line, while colored lines represent fitted regression line.



28 **Supplementary Fig. 4** | Sensitivity analysis of our mass balance to potential variability in  $k_{600}$  models for  
29 AWD. **A)** The x-axis shows the average wind speeds at 10 m, and the y-axis shows the corresponding  $k_{600}$   
30 derived from four different models: MacIntyre et al. (2010; based on eddy covariance estimates, mixed  
31 buoyancy-derived), Cole and Caraco (1998), and Crusius and Wanninkhof (2003) (both derived from wind  
32 speed based on SF<sub>6</sub> tracer experiments). The colored lines represent smoother fits **B)** The x-axis shows  
33  $OMP_V$  estimates in this study using the  $k_{600}$  model derived from Vachon and Prairie (2013; based on lake  
34 size and wind speed). The y-axis shows estimates adjusted using the three alternative models. The black  
35 line indicates the 1:1 line, while colored lines represent fitted regression lines. **C)** Boxplots illustrate the  
36 variability in  $OMP_V$  derived from each model as a function of total biomass volume of cyanobacteria, and **D)**  
37 as a function of PAR absorbed by cyanobacteria and algae. Boxes show the 1<sup>st</sup> and 3<sup>rd</sup> quartile with the  
38 median (white line), whiskers extend to most extreme data point within 1.5 times the IQR from the box.

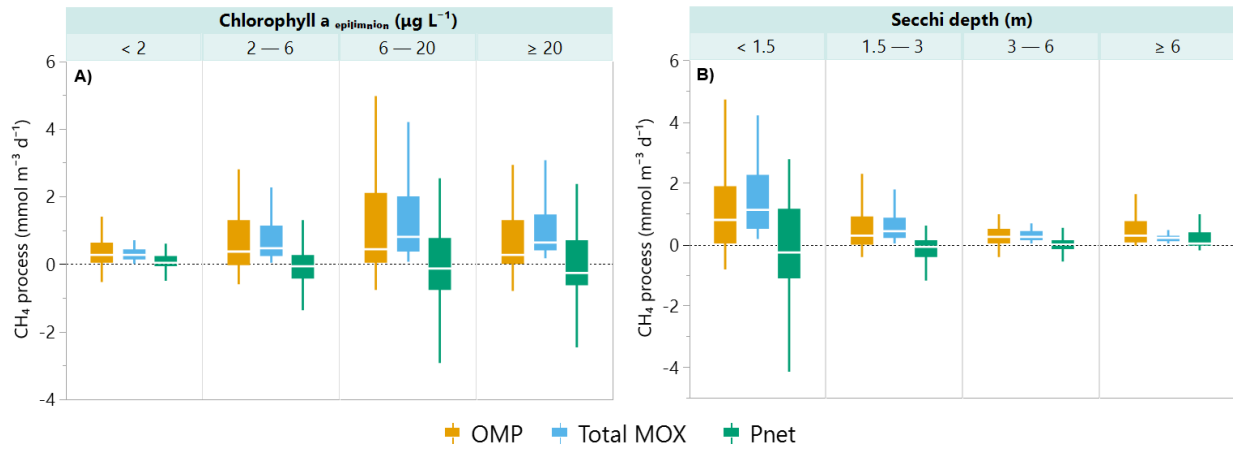
39



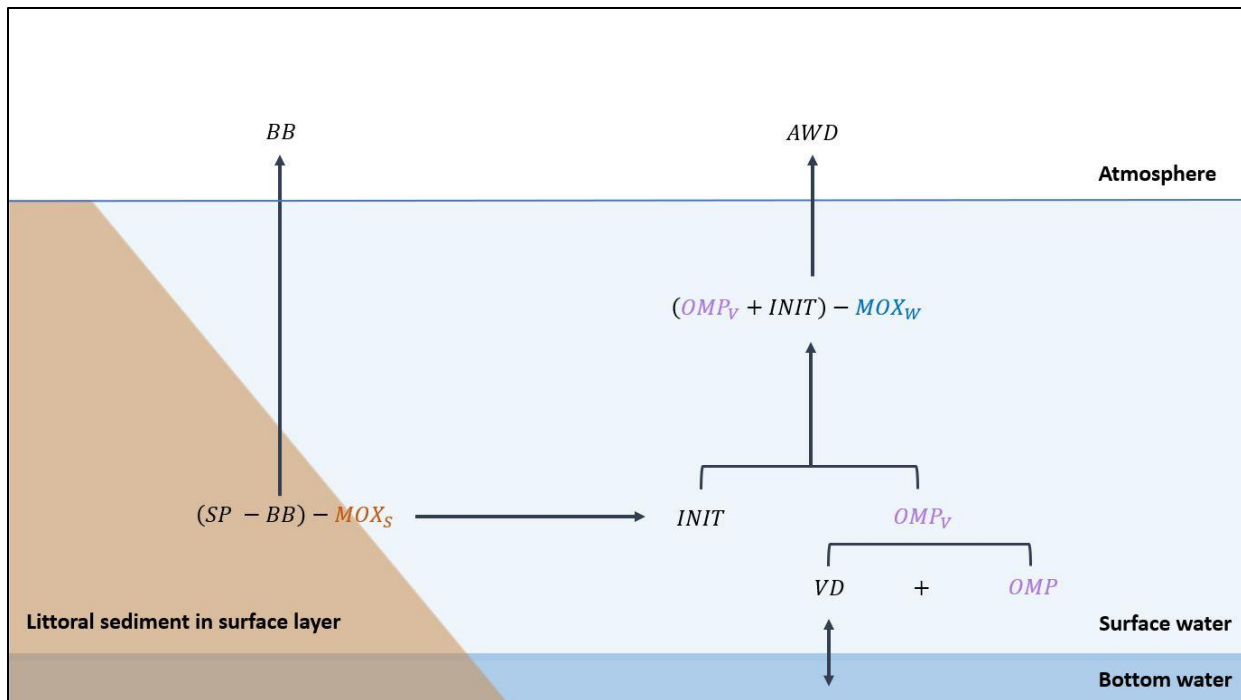
40

41 **Supplementary Fig. 5 |** Sensitivity analysis of our mass balance to potential variability in  $MOX_W$ . The x-  
 42 axis shows  $OMP_V$  estimates assuming  $MOX_W$  derived from aerobic oxidation kinetics that integrate the  
 43 effects of surface  $CH_4$ ,  $O_2$ , and temperature, following Thottathil et al. (2019), while the y-axis shows  
 44 corresponding estimates when  $MOX_W$  is adjusted to  $\pm 15\%$ ,  $\pm 30\%$ , and  $\pm 70\%$ , respectively. The black line  
 45 indicates the 1:1 line, while colored lines represent fitted regression line.

46



49 **Supplementary Fig. 6 |** Boxplots illustrate the variability in  $\text{OMP}_V$ , total MOX (as sum of  $\text{MOX}_S$  and  $\text{MOX}_W$ ),  
50 and  $P_{net}$  (all rates are normalized to surface-water volume) as a function of **A)** chlorophyll a (in  $\mu\text{g L}^{-1}$ ) and  
51 **B)** Secchi depth (in m) in surface layers. Boxes show the 1<sup>st</sup> and 3<sup>rd</sup> quartile with the median (white line),  
52 whiskers extend to most extreme data point within 1.5 times the IQR from the box.



53

54 **Supplementary Fig. 7 |** Conceptual schematic of the extended mass balance approach. CH<sub>4</sub> mass balance  
 55 components (in mol d<sup>-1</sup>) in surface water and littoral sediment: sedimentary CH<sub>4</sub> production (SP), ebullitive  
 56 CH<sub>4</sub> emission (BB), air-water diffusive CH<sub>4</sub> emission to the atmosphere (AWD), CH<sub>4</sub> oxidized at the  
 57 sediment-water interface (MOX<sub>S</sub>), CH<sub>4</sub> oxidized in surface waters (MOX<sub>W</sub>), CH<sub>4</sub> reaching the water column  
 58 after MOX<sub>S</sub> (INIT), vertical CH<sub>4</sub> diffusion between surface and bottom water layers (VD), oxic CH<sub>4</sub>  
 59 production (OMP), and the net CH<sub>4</sub> as sum of OMP and VD (OMP<sub>V</sub>).

60      **Detailed calculations to derive equation (11) in the extended mass balance approach**

61

62      In the main context, equations (2) – (10) were then sequentially combined to derive an integrative function  
63      of the unknown  $MOX_S$  (i.e., equation (11)) as follows.

64      In equation (8), isolate the unknown  $\delta^{13}C_{INIT}$ .

65      **SEq 1**

66      
$$\delta^{13}C_{INIT} = \left( \frac{SP - BB - MOX_S}{SP - BB} \right)^{\frac{1-\alpha}{\alpha}} \cdot (\delta^{13}C_{SED} + 1000) - 1000$$

67      In equation (10),  $frac_{INIT}$  is the fraction of  $INIT$  and defined as  $\frac{INIT}{INIT + OMP_V}$ . Then, substitute equation (7)  
68      into this,

69      **SEq 2**

70      
$$frac_{INIT} = \frac{AWD + MOX_w - OMP_V}{AWD + MOX_w}$$

71      Substitute SEq 1 and SEq 2 into equation (10).

72      **SEq 3**

73      
$$\delta^{13}C_{INIT+OMP} = \left( \frac{AWD + MOX_w - OMP_V}{AWD + MOX_w} \right) \times \left\{ \left( \frac{SP - BB - MOX_S}{SP - BB} \right)^{\frac{1-\alpha}{\alpha}} \cdot (\delta^{13}C_{SED} + 1000) - 1000 \right\}$$

74      
$$+ \left( \frac{OMP_V}{AWD + MOX_w} \right) \times \delta^{13}C_{OMP_V}$$

75      Similarly, in equation (9), isolate the unknown  $\delta^{13}C_{INIT+OMP_V}$ .

76      **SEq 4**

77      
$$\delta^{13}C_{INIT+OMP_V} = \frac{(\delta^{13}C_{SURF} + 1000)}{\left( \frac{OMP_V + INIT - MOX_w}{OMP_V + INIT} \right)^{\frac{1-\alpha}{\alpha}}} - 1000$$

78      Substitute equation (7) into SEq 4.

79 **SEq 5**

$$80 \quad \delta^{13}C_{INIT+OMP_V} = \frac{(\delta^{13}C_{SURF} + 1000)}{\left(\frac{AWD}{AWD + MOX_w}\right)^{\frac{1-\alpha}{\alpha}}} - 1000$$

81 Let SEq 3 equal SEq 5.

82 **SEq 6**

$$83 \quad \frac{(\delta^{13}C_{SURF} + 1000)}{\left(\frac{AWD}{AWD + MOX_w}\right)^{\frac{1-\alpha}{\alpha}}} - 1000$$
$$84 \quad = \left(\frac{AWD + MOX_w - OMP_V}{AWD + MOX_w}\right) \times \left\{ \left(\frac{SP - BB - MOX_S}{SP - BB}\right)^{\frac{1-\alpha}{\alpha}} \cdot (\delta^{13}C_{SED} + 1000) - 1000 \right\}$$
$$85 \quad + \left(\frac{OMP_V}{AWD + MOX_w}\right) \times \delta^{13}C_{OMP_V}$$

86 Rearrange equation (2) as  $AWD + MOX_w - OMP_V = SP - BB - MOX_S$ . Then, substitute this into SEq 6.

87 **SEq 7**

$$88 \quad \frac{(\delta^{13}C_{SURF} + 1000)}{\left(\frac{AWD}{AWD + MOX_w}\right)^{\frac{1-\alpha}{\alpha}}} - 1000$$
$$89 \quad = \left(\frac{SP - BB - MOX_S}{AWD + MOX_w}\right) \times \left\{ \left(\frac{SP - BB - MOX_S}{SP - BB}\right)^{\frac{1-\alpha}{\alpha}} \cdot (\delta^{13}C_{SED} + 1000) - 1000 \right\}$$
$$90 \quad + \left(\frac{OMP_V}{AWD + MOX_w}\right) \times \delta^{13}C_{OMP_V}$$

91 In SEq 7, isolate the unknown  $OMP_V$ .

92 **SEq 8**

$$93 \quad OMP_V = \left[ \frac{\delta^{13}C_{SURF} + 1000}{\left( \frac{AWD}{AWD + MOX_W} \right)^{\frac{1-\alpha}{\alpha}}} - 1000 - \left( \frac{SP - BB - MOX_S}{AWD + MOX_W} \right) \right]$$

$$94 \quad \cdot \left\{ \left( \frac{SP - BB - MOX_S}{SP - BB} \right)^{\frac{1-\alpha}{\alpha}} \cdot (\delta^{13}C_{SED} + 1000) - 1000 \right\} \cdot \frac{AWD + MOX_W}{\delta^{13}C_{OMP_V}}$$

95 Rearrange equation (2) as  $OMP_V = AWD + MOX_W - SP + BB + MOX_S$ . Then, let this equal SEq 8.

96 **SEq 9**

$$97 \quad AWD + MOX_W - SP + BB + MOX_S$$

$$98 \quad = \left[ \frac{\delta^{13}C_{SURF} + 1000}{\left( \frac{AWD}{AWD + MOX_W} \right)^{\frac{1-\alpha}{\alpha}}} - 1000 - \left( \frac{SP - BB - MOX_S}{AWD + MOX_W} \right) \right]$$

$$99 \quad \cdot \left\{ \left( \frac{SP - BB - MOX_S}{SP - BB} \right)^{\frac{1-\alpha}{\alpha}} \cdot (\delta^{13}C_{SED} + 1000) - 1000 \right\} \cdot \frac{AWD + MOX_W}{\delta^{13}C_{OMP_V}}$$

100 In the left-hand side of SEq 9, move all variables except  $MOX_S$  to the right-hand side. Then, finally it  
101 derives an integrative function as equation (11), in which  $MOX_S$  appears on both sides.

102 **SEq 10 (i.e., equation (11) in the main manuscript)**

$$103 \quad MOX_S = \left[ \frac{\delta^{13}C_{SURF} + 1000}{\left( \frac{AWD}{AWD + MOX_W} \right)^{\frac{1-\alpha}{\alpha}}} - 1000 - \left( \frac{SP - BB - MOX_S}{AWD + MOX_W} \right) \right]$$

$$104 \quad \cdot \left\{ \left( \frac{SP - BB - MOX_S}{SP - BB} \right)^{\frac{1-\alpha}{\alpha}} \cdot (\delta^{13}C_{SED} + 1000) - 1000 \right\} \cdot \frac{AWD + MOX_W}{\delta^{13}C_{OMP_V}} - AWD - MOX_W$$

$$105 \quad + (SP - BB)$$

106

107 Due to its nonlinear form,  $MOX_S$  can be solved numerically using an iterative method. Lastly, substituting  
108 the calculated  $MOX_S$  into equation (2) yielded  $OMP_V$  as

109 **SEq 11 (i.e., equation (12) in the main manuscript)**

110 
$$OMP_V = AWD - (SP - BB) + MOX_S + MOX_W$$